EUROPEAN FUSION DEVELOPMENT AGREEMENT

EFDA–JET–CP(01)08-02

V.G.Kiptily, F.E.Cecil, O.N.Jarvis, M.J.Mantsinen, S.E.Sharapov,
L.Bertalot, S.Conroy, L.C.Ingesson, K.D.Lawson, S.Popovichev
and JET EFDA Contributors

Gamma-ray Diagnostics of Energetic Ions in JET

Gamma-ray Diagnostics of Energetic Ions in JET

V.G.Kiptily, F.E.Cecil[1], O.N.Jarvis, M.J.Mantsinen[2], S.E.Sharapov, L.Bertalot[3], S.Conroy[4], L.C.Ingesson[5], K.D.Lawson, S.Popovichev and JET EFDA Contributors

EURATOM-UKAEA Fusion Association, Culham Science Centre, Abingdon, OX14 4XB, United Kingdom.

[1]*Department of Physics, Colorado School of Mines, Golden, Colorado 80401, USA*

[2]*Helsinki University of Technology, Association Euratom-Tekes, P.O.Box 2200, FIN-02015 HUT, Finland*

[3]*Ass. Euratom/ENEA/CNR sulla Fusione, Centro Ricerche Energia ENEA-Frascati 00044 Frascati, Rome*

[4]*INF, Uppsala University, Euratom-VR Association, Box 535, 75 121 Uppsala, Sweden*

[5]FOM-Inst. Plasmafysica "Rijnhuizen", Ass. Euratom-FOM, TEC, PO Box 1207, 3430 BE Nieuwegein, NL

**See Annex of J. Pamela et al., "Overview of Recent JET Results and Future Perspectives", Fusion Energy 2000 (Proc. 18th Int. Conf. Sorrento, 2000), IAEA, Vienna (2001).*

Preprint of Paper to be submitted for publication in Proceedings of the 7th IAEA TCM on Energetic Particles, (Gothenburg, 8-11 October 2001)

‘‘This document is intended for publication in the open literature. It is made available on the understanding that it may not be further circulated and extracts or references may not be published prior to publication of the original when applicable, or without the consent of the Publications Officer, EFDA, Culham Science Centre, Abingdon, Oxon, OX14 3DB, UK.”

“Enquiries about Copyright and reproduction should be addressed to the Publications Officer, EFDA, Culham Science Centre, Abingdon, Oxon, OX14 3DB, UK.”

ABSTRACT

An overview of recent gamma-ray diagnostic measurements of energetic ions in JET is presented. Observations of nuclear reaction gamma rays involving ^3He and H minority ICRF-heating-ions and other fuel elements and plasma impurities are presented and analysed. Further development of the gamma-diagnostics is discussed.

1. INTRODUCTION

Investigation of fast ion production during auxiliary heating and of the subsequent fast ion behaviour in magnetically confined plasmas, together with an evaluation of the resulting bulk ion heating efficiency, are of a crucial importance for fusion reactor development. One of the techniques capable of studying fast ions is fusion γ-ray diagnostics as first proposed by Medley and Hendel [1]. Measurements performed on DIII-D [2], TFTR [3], JET [4] and JT-60U [5] tokamaks have shown that intense gamma-ray emission is produced by fast particles (fusion products, ICRF-driven ions) when they react with plasma fuel ions and with the main plasma impurities (beryllium, boron, carbon, oxygen). Gamma-ray energy spectra recorded with collimated spectrometers provide information on the line-integrated energy distribution functions of the fast ions which exist in the plasma. An effective temperature of the fast ions can be deduced due to the fact that, as rule, the reaction excitation functions are well established and exhibit a threshold or/and resonant nature.

While the measurements of the intensity of an individual line in a spectrum is determined by the energy of the reacting particles (projectile and target), it is not possible to determine the velocities or pitch angles distribution of the fast particles; consequently, trapped and passed ions can not be distinguished. However, the pitch angle distribution could be measured by means of high energy resolution spectrometry capable of measuring the Doppler broadening of the γ-ray lines [6].

In addition, the spatial distribution of the fast ions in a plasma is of an interest. Gamma-ray emission profile measurements provide data on spatial distributions of radiation sources that are produced by the particles due to nuclear reactions.

Gamma-ray emission from JET plasmas has been systematically measured since being first reported by Boyd et al [7]. Different physics effects arising during ICRF and NBI heating in the JET tokamak have been successfully interpreted using these γ-ray measurements [4,7-9]. The main part of results described in present paper is based on γ-ray measurements made in the 2000-2001 JET campaign. In the recent experiments the possibly ITER-relevant ICRH scenarios $(^3He)D$ and $(^3He)^4He$ have been studied. A special ^4He-plasma experiment with third harmonic ICRF-heating of ^4He-beams has demonstrated the possibility of alpha-particle investigation in a non activated operation in future devices. Results of measurements H- and D-tails during H-minority heating are discussed. An example of H-minority heating in DT-plasma is demonstrated.

2. EXPERIMENTAL EQUIPMENT

Gamma-ray energy spectra were recorded with a calibrated bismuth germanate (BGO) scintillation detector (75 mm x 75 mm). This detector is located in a well-shielded bunker behind the X-ray

crystal spectrometer and views the plasma tangentially. In order to reduce neutron flux and γ-ray background the front collimator was filled to a depth of 500 mm with polythene. Behind the BGO-detector there is a dump plug consisting of polythene of length 500mm and a final plug of lead of length 500mm. The detector line-of-sight lies in a horizontal plane about 30 cm below the plasma axis. The γ-rays are recorded in the energy range 1-28MeV with an energy resolution of about 4% at 10MeV. In some experiments a 125-diam x 125-mm-long NaI(Tl) scintillation detector located in the JET roof laboratory was used to view the plasma vertically through the centre (R = 2.95m).

The spatial distribution of gamma-ray emission sources in the plasma were measured in the ^4He-plasma experiments only, because of suitably low neutron and γ-ray background conditions. Gamma-ray profiles have been recorded by means of the JET profile monitor [10] which is routinely used for neutron measurements (Fig.1). It consists of two cameras, vertical and horizontal with 9 and 10 line-of-sights respectively. The radiation detectors are NE213 liquid scintillators dedicated for neutron measurements. Gamma-ray measurements are possible due to the fact that neutron and γ events are electronically separated by exploiting the different pulse shape characteristics for the two forms of radiation. The standard pulse shape discrimination modules were set up to restrict the detection of γ-ray emission to the energy range from 1.8 to 6MeV.

3. ANALYSIS

3.1 SIMULATION OF GAMMA-RAY SPECTRA

In order to infer an effective temperature of the fast ions from experimental data a dedicated code for γ-ray spectrum modelling, GAMMOD, has been developed. The program is based on known reaction cross-section data and includes almost a hundred γ-ray transitions in the final nuclei. The list of nuclear reactions used in the code are given in Table 1. The program includes the response functions, calculated *a priori*, for the gamma spectrometer and natural background spectrum. Experimental data for the time-averaged plasma temperature, the applied NBI power, fuel and impurity densities are used as input parameters.

The modelled spectrum consists of three contributions:

i) a continuous background arising from inelastic scattering and radiative capture of neutrons;

ii) the spectrum from nuclear reactions between fusion products and main low-Z impurities (discharges with NBI heating);

iii) the spectrum produced by fast ions accelerated during ICRF heating due to reactions with impurities.

Analytically the combined energy spectrum may be expressed as

$$S(E_\gamma) \propto \sum_m \sum_k \sum_i \int R_{m,k}(E_\gamma, E_i, E_f)\, n_z^{(m)}\, n_f^{(k)}\, F_k(T_{eff}^{(k)}, E_f) \sigma_{m,k}(E_f) V_k(E_f) dE_f + B(E_\gamma),$$

where $R_{m,k}(E_\gamma, E_i, E_f)$ is the spectrometer response function for gamma-rays with energy E_i produced

in the nuclear reaction between the target m and the fast particle k at energy Ef; $n_z^{(m)}$, $n_f^{(k)}$ are densities of the target ions and fast particles; $F_k(T_{eff}^{(k)}, E_f)$ is the energy distribution function at effective temperature $T_{eff}^{(k)}$; $\sigma_{m,k}(E_f)$, $V_k(E_f)$ are the cross section of reaction and velocity of fast particle; $B(E_\gamma)$ is a γ-ray background.

The continuous backgrounds depend almost entirely on neutron rate. Energy distributions of the fusion products have been approximated by the classical distribution functions for steady-state plasmas. A Maxwellian energy distribution is chosen to describe the line-of-sight averaged ICRF-driven ions' tail. The analysis of recorded gamma-ray spectra using GAMMOD gives the effective tail temperatures, the fast ions' concentrations and the contribution to the neutron yield made by the fast particles.

The feasibility and accuracy of the modelling results depend on the quality of the recorded spectra, uncertainties of input plasma parameters and computational uncertainties. In general, plasma data used in calculations have experimental uncertainties below 10% with the exception of the low-Z impurities concentrations. These main parameters in the code are determined with accuracy around 20%. An important problem is nuclear cross section data; specifically gaps in the data and the consequent extrapolations for some reaction which may result in significant uncertainties in the deduced plasma parameters. Nevertheless, a crosscheck of results and the number of γ-lines in the spectrum due to several reactions will allow reliability of the results to be improved. An average accuracy of the effective tail temperature deduced from the γ-ray spectrum can be estimated at around 30%. In this case, a simple function chosen for the approximation of fast ions distribution introduces a negligible error compared to the other sources of uncertainty.

3.2. GAMMA-RAY TOMOGRAPHY

The same tomography method as used for bolometer and soft x-ray tomography was applied to the γ-ray data [11]. The method uses anisotropic smoothness on flux surfaces as objective function, i.e. *a priori* physical information about the expected emission profile. A feature of this method, and most other tomography methods due to the very nature of ill-posed problems with noisy data, is that the solution found is nearly always smoother than the actual emission profile. Because of this, we can be almost certain that the actual emission profile will not be less peaked than the found solution, nor will it have other major features that are not present in the found solution. It is important to realise this fact when considering the physical implications of the tomographic reconstructions.

The KN3 system has only two fairly coarse views of the plasma. Therefore, the reconstructions will only show general features of the emission profile; information is simply not available to do better unless more *a priori* knowledge is available about the emission profiles. In this reconstruction method the quality of the fit to the measurements is an input parameter controlled by the estimated errors.

4. RESULTS

4.1. GAMMA-RAY OBSERVATION DURING ^{3}HE-MINORITY HEATING

A phenomenon which could be explained in terms of an ICRF-pinch [12, 13] has been observed by means of the γ-ray measurements in JET both in *D* and ^4He plasma with ^3He-minority ICRF heating. First, in deuterium plasmas, γ-ray emission with asymmetric ICRF wave heating which was recorded by two spectrometers viewing the plasma along horizontal and vertical lines of sight. Depending on the toroidal direction in which the launched wave propagates, co-current ($+90^o$ phasing) or counter-current (-90^o phasing) the resulting spatial pinch of the trapped ions is either inwards (Pulse No: 51646) or outwards (Pulse No: 51645). Figure 2 shows the relative γ-ray intensity recorded with detector viewing through the centre of plasma is much higher during the Pulse No: 51646 ($+90^o$ phasing) in comparison with Pulse No: 51645 (-90^o phasing). This could be interpreted as a formation of the trapped ions' inward pinch when ICRF wave propagates in co-current direction.

To further study the γ-ray emission profiles in the presence of asymmetric ICRF, recent experiments with ^4He plasmas [14] demonstrated possible evidence for ICRF-induced ^3He-minority pinch. Tomographic reconstructions have been made of the recorded γ-ray emission profiles in discharges Pulse No: 54239 ($+90^o$ phasing) and Pulse No: 54243 (-90^o phasing) (Fig.3a). To properly assess the reliability of the tomography, the technique of varying reconstruction parameters within a reasonable range as described in [11] was used to establish regions of confidence in the cross-sections (Fig. 3b). The most significant contributor to the region of uncertainty is the variation of measurements to three times their standard deviation. Thus, the profound differences of the γ-ray emission profile between the two discharges are beyond doubt. The profile in 54239 is rather flat and centred at the magnetic axis, whereas the profile in 54243 is much lower and centred around the ^3He-minority resonance layer. Figure 3 shows different spatial distributions of the radiation due to nuclear reactions between fast ^3He-ions and carbon, which was the main impurity in JET. The disparity is due to the differing type of the fast ^3He ion orbits for two ICRF phasings. A qualitative analysis of the emission profile is consistent with the results of measurements in deuterium plasmas. As predicted [15], the resulting spatial pinch of the trapped ions should be inwards for the shot Pulse No: 54239 and outwards for other one.

An analysis of the γ-ray energy spectra recorded in these discharges indicates that the γ-radiation is mainly produced by the threshold nuclear reaction $^{12}C(^3He,p\gamma)^{14}N$ and the effective temperature of the ICRF accelerated ^3He ions is $\langle T_{eff} \rangle = 650 \pm 150$keV. In the case of Pulse No: 54243 with the opposite phasing (-90^o) $\langle T_{eff} \rangle$ is roughly the same, but the total γ-radiation intensity is halved. Experimental and modelled γ-ray spectra are compared in Fig. 4 (left) for Pulse No: 54239, with $+90^o$ -phasing. It is found that the reaction yield goes up from the 'threshold temperature' (around 300keV) to the maximal one with characteristic time equal to 0.2s as shown in Fig.4 (right). This value is consistent with the thermalization time [16]

$$\tau_{th} = \frac{\tau_{se}}{3} \ln[1 + (E_f / E_{crit})^{3/2}] \approx 0.25s$$

where E_f is energy of fast ions and E_{crit} is known as fast-ion critical energy.

The sensitivity of the γ-ray spectra to increasing ^3He-puff is demonstrated in Fig.5 By increasing the ^3He-puff, the effective temperature of the ions is decreased which is consistent with lower fraction of the power absorbed by ^3He and increase in the direct electron damping [13].

Strong emission from $^{12}C(d,p\gamma)^{13}C$ and observation of the 17-MeV γ-rays from the reaction $D(^3He, \bullet)\ 5\ Li$ in Pulse Nos: 53818, 53819 and 53820 have been observed (Fig.6). In these shots, ICRF power was absorbed at the fundamental D-resonance (R = 2.4m) and fundamental ^3He-resonance (R = 3.3m). It is found out the effective temperature of ^3He-tail is much below 100 keV whereas D-tail is around 300keV. The low energy ^3He-tail is connected with a high ^3He-concentration that is near the optimal for the mode conversion when the direct electron damping is predominant. Relatively high yield of the reaction $D(^3He,\gamma)^5Li$ which is a weak branch of reaction $D(^3He,p)^4He$ in these shots can be explained by high energy D-tail and high density of ^3He. Furthermore, high energy protons (E_p>5MeV) have been observed due to the threshold reaction $^{12}C(p,p,\gamma)^{12}$C, giving rise a peak of γ-ray intensity at energy 4.44MeV. The reaction $D(^3He,p)^4He$ is the likely source of the energetic protons (15MeV) in these shots.

4.2. ACCELERATION OF ^{4}HE-BEAM IN ^{4}HE-PLASMA

In a dedicated JET experiment [13], during third harmonic heating of ^4He-plasma in the presence of ^4He-beams (120keV and/or 70keV), γ-radiation due to reaction $^9Be(\alpha,n\gamma)^{12}C$ was observed for the first time. This reaction has been proposed previously as a dedicated diagnostic for fusion alpha-particles [6]. Excitation functions of the first two levels in the final nucleus ^{12}C have a resonance pattern (Fig.7) that is helpful for the analysis.

Gamma-ray spectrum simulation indicates the acceleration of ^4He ions up to energies in excess 2MeV. An example of measured and calculated spectra is presented in Fig.8 for Pulse No: 54168. The result of the spectrum modelling is $<T_{eff}>^4$He = 1.30.4MeV. This calculation is based on an assumption that ratio of impurity concentrations ^{9}Be/^{12}C is about 1.5% which is in the range suggested by visible, VUV and XUV spectroscopy for this ratio. As the ^4He-beam energy was increased from 70-keV to 120keV, the estimated effective temperature $<T_{eff}>^4$He increased from 0.5±0.2MeV up to 1.1±0.4MeV.

Observation of strong γ-ray emission from $^{12}C(d,p\gamma)^{13}C$ in all shots shows that some ICRF power was also absorbed at the third harmonic D-resonance. The modelling shows in the low-energy beam discharge that the fast D-component is around 6% of the ^4He one, whereas in the discharge with 120-keV beam it is about 3%. The effective temperature in these shots was assessed as $<T_{eff}> \approx$ 0.4MeV. Gamma-ray modelling facilitates the interpretation of the neutron yield produced by the fast particles during low-neutron-yield discharges. In ^4He-discharges, as in Pulse No: 54168, the fast D-component is a few percent of the ^4He-ion component; nevertheless, the accelerated deuterons provide around 90% of the neutron yield due to higher *d-d* fusion cross section in comparison with $^9Be(\alpha,n\gamma)^{12}$C.

4.3. ACCELERATION OF *H* AND *D* AT $\omega = \omega_{CH} = 2\omega_{CD}$

Among the diagnostic nuclear reactions with protons which can take place in JET plasmas (see Table 1), the reaction $D(p,\gamma)^3He$ is useful for analysis of low-energy tail distributions. First observations of 5.5-MeV gammas from this reaction was in experiment performed with neutral hydrogen beam at Doublet-III [2]. In JET, these gammas have been recorded during experiments with ICRF heating [17].

In recent experiments during H-minority heating of deuterium plasma, γ-ray emission from $D(p,\gamma)^3He$ has been recorded and the effective temperature of the hydrogen tail was assessed. With the assumption of the Maxwellian distribution function for the RF-accelerated ions and bulk deuterium, most reactions occur at energy of the Gamow peak $E_\gamma = Q + E_G$, forming a symmetric distribution with a width of

$$\Delta E_{fwhm} \text{ - } \hat{}16E_G \quad \frac{<T_{Dp}>}{3} + 81n2 \quad \frac{Q^2}{M_{3He}}<T_{Dp}> \quad (MeV),$$

where $E_G \approx 0.74 <T_{Dp}>^{2/3}$ (MeV); $<T_{Dp}>$ (MeV) is effective temperature of reactants; $Q = M_H + M_D - M_{3He}$ (MeV) is the energy of reaction equal to 5.5MeV; M_i are masses of *H*, *D* and ^{3}He. Here the width ΔE_{fwhm} includes the Gamow peak width and Doppler broadening.

A typical spectrum measured during the H-minority heating in deuterium Pulse No: 50659 is shown in Fig.9. The maximum energy of the γ-rays from the capture reaction $D(p,\gamma)^3He$ is about 5.83MeV. According to the assessments performed using GAMMOD, the effective temperature of the hydrogen minority the $<T_{eff}>_H$ was found to be 0.20±0.05MeV. The deuterium-tail is around 0.1MeV, and the population is three times lower than hydrogen fast component. In this shot, the *H*-resonance which coincides with the second harmonic *D*-resonance, was near the centre of plasma at R = 2.93m. Apparently, the fast deuterium population is due to damping of ICRF power at $\omega = 2\omega_{CD}$. The total neutron rate has similar time behaviour as the γ-ray count rate.

An obvious case when the gamma-ray spectrum indicates an energetic *H*-tail during ICRH heating is shown in Fig.10. Gamma-rays from the threshold reaction $^{12}C(p,p,\gamma)^{12}C$ have been observed. According to the spectrum simulation the effective temperature of H-minority was assessed as $<T_{eff}>_H \approx 2.6$MeV. In this shot the first (4.44MeV) and second (7.65MeV) levels of nucleus ^{12}C were excited by energetic hydrogen ions. The Doppler broadening of the 4.44-MeV peak is likewise seen in comparison with the detector respond function. And again, the neutron timing behaviour is the similar to the γ-ray signal. The Pulse No: 51809 as Pulse No: 50659 discussed above has the *H*-resonance and second harmonic *D*-resonance in the plasma at R = 2.86m and, obviously, the neutron yield behaviour can be explained by *D* damping.

Typical γ-spectrum recorded in the deuterium-tritium JET campaign (Fig.11), DTE1, which demonstrates the γ-ray emission due to the reaction $^{12}C(p,p,\gamma)^{12}$C, indicates the presence of ICRF-accelerated protons with energy exceeding 5MeV. For this tritium Pulse No: 41759 the effective tail temperature of ICRF-driven *H*-ions is estimated to be in the range 0.4 to 0.6MeV. This

allows the identification of the threshold reaction $T(p,n)^3He$ as the source of 40% excess neutron emission [18]. Since there is no indication of gamma rays due the reaction $^{12}C(d,p\gamma)^{13}C$ in the measured γ-spectrum, the surprisingly high neutron yield in this discharge cannot be due to the second-harmonic-accelerated D-ions. That the contribution to the neutron yield from the knock-on effect is negligible is supported by neutron measurements and high-energy neutral particle analyser data [19].

CONCLUSIONS

The capabilities of the γ-ray diagnostics for studies of fast ion behaviour in deuterium, hydrogen, helium and tritium plasmas have been demonstrated. Gamma-ray spectrometry and profile measurements provide information on the energy and spatial particle distribution of the fast ions and the efficiency of ICRF heating of bulk plasma. Further development of γ-ray spectrum modelling and the extension of the nuclear reaction data-base is essential. New possibilities of γ-ray diagnostics for fast confined alpha-particle investigation have been shown in a ^4He-plasma experiment. The nuclear reaction $^9Be(\alpha,n\gamma)^{12}C$ could be useful not only for *D*T-plasma but also in a possible *H*e-phase of ITER. In this case, high-energy resolution spectrometers could provide additional information due to the possibility of measuring the Doppler-broadening of the γ-lines.

ACKNOWLEDGEMENTS

This work has been conducted under the European Fusion Development Agreement and in collaboration with Department of Physics of the Colorado School of Mines (USA), and is partly funded by Euratom and the UK Department of Trade and Industry.

REFERENCES

[1]. S.S.Medley, H.Hendel, Bull. Am. Phys. Soc. 26 (1982) 980.
[2]. D.E.Newman, F.E.Cecil, Nucl. Instrum. Methods **227** (1984) 339.
[3]. F.E.Cecil, S.S.Medley, Nucl. Instrum. Methods **271** (1988) 628.
[4]. G.J.Sadler, S.W.Conroy, O.N.Jarvis, et al., Fusion Technology **1**8, (1990) 556.
[5]. T.Kondoh et al., J. Nucl. Mat. **241-243** (1997) 564.
[6]. V.G.Kiptily, Fusion Technology **18** (1990) 583.
[7]. D.A.Boyd, D.J.Campbell, J.G.Cordey, et al., Nucl. Fusion **29** (1989) 593.
[8]. J.Jacquinot, G.J.Sadler, Fusion Technology **2**1, (1992) 2254.
[9]. O.N.Jarvis, J.M.Adams, P.J.A.Howarth, et al., Nucl. Fusion **36** (1996) 1513.
[10]. J.M.Adams, O.N.Jarvis, G.J.Sadler, D.B.Syme, N.Watkins, Nucl. Instrum. Methods Phys. Res. **A239** (1993) 277.
[11]. L.C.Ingesson et al., Nucl. Fusion **38** (1998)1675
[12]. L.Chen, J.Vaclavik, G.W.Hammett, Nucl. Fusion **28** (1988) 389.
[13]. L.-G.Eriksson, et al., Phys. Rev. Lett. **81** (1998) 1231 .

[14]. M.J.Mantsinen et al., ICRF heating scenarios in JET with emphasis on He plasmas for the non-activated phase of ITER, 14th Topical Conference on Radio Frequency Power in Plasmas, Oxnard, 7-9 May 2001.
[15]. T.Johnson et al., RF-induced Pinch of Resonant 3 He Minority Ions in JET 14th Topical Conference on Radio Frequency Power in Plasmas, Oxnard, 7-9 May 2001.
[16]. T.H.Stix, Nucl. Fusion **15** (1975) 737.
[17]. F.E.Cecil, P.van Belle, O.N.Jarvis, G.J.Sadler, JET-IR(94)04.
[18]. M.J.Mantsinen, O.N.Jarvis, V.G.Kiptily et al., First Observation of *p-T* Fusion in JET Tritium Plasmas with ICRF Heating of Protons, Nucl. Fusion (in press).
[19]. A.A.Korotkov, A.Gondhalecar, A.J.Stuart, Nucl. Fusion **33** (1997) 35.

Reaction	Reaction Energy, MeV	Reaction	Reaction Energy, MeV
$D(p,\gamma)^3He$	5.5	$^9Be(p,\gamma)^{10}B$	6.586
$D(d,p)^3H$	4.033	$^9Be(p,p'\gamma)^9Be$	−2.429
$D(d,n)^3He$	3.269	$^9Be(p,\alpha\,\gamma)^6Li$	2.125
$D(d,\gamma)^4He$	23.84	$^9Be(d,p\gamma)^{10}Be$	4.587
$D(t,n)^4He$	17.59	$^9Be(d,n\gamma)^{10}B$	4.36
$D(t,\gamma)^5He$	16.63	$^9Be(t,n\gamma)^{11}B$	9.56
$D(^3He,p)^4He$	18.354	$^9Be(^3He,p\gamma)^{11}B$	10.322
$D(^3He,\gamma)^5Li$	16.38	$^9Be(^3He,n\gamma)^{11}C$	7.557
$T(p,n)^3He$	−0.7637	$^9Be(^3He,d\gamma)^{10}B$	1.09
$T(p,\gamma)^4He$	19.814	$^9Be(^4He,n\gamma)^{12}C$	5.701
		$^{12}C(p,p'\gamma)^{12}C$	−4.44
		$^{12}C(d,p\gamma)^{13}C$	2.722
		$^{12}C(3He,p\gamma)^{14}N$	4.779

Table 1: *Nuclear reactions used for gamma-ray spectrum modelling*

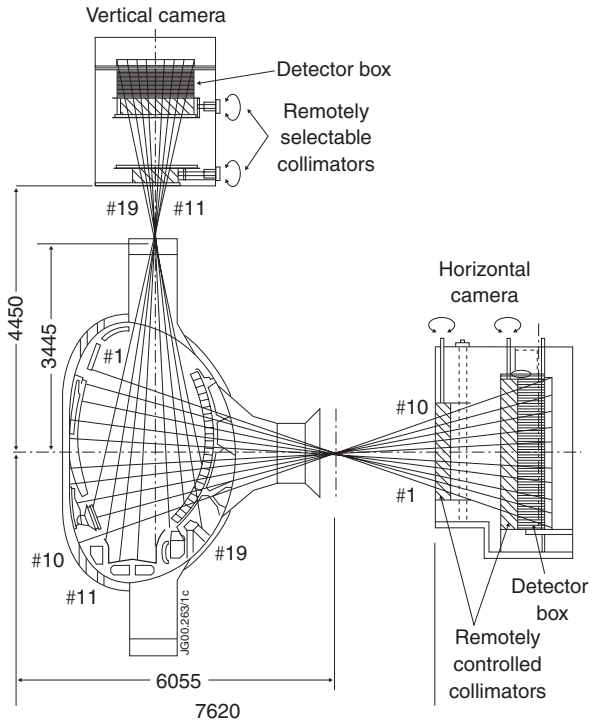

Figure 1: Scheme of the JET neutron emission profile monitor used for the spatial ray emissivity measurements.

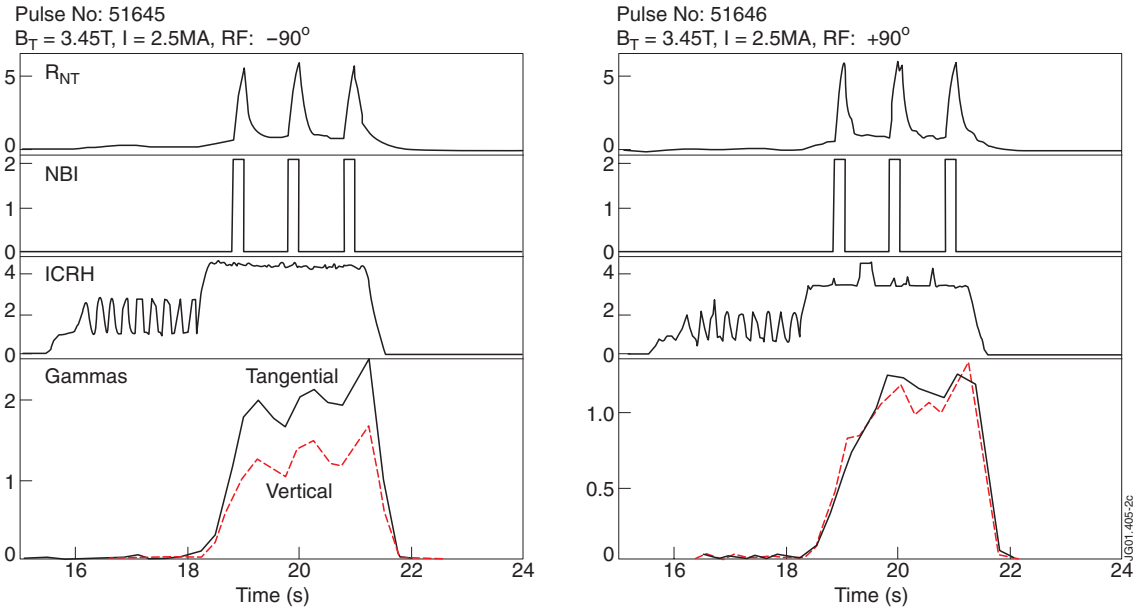

Figure 2: Overview of two discharges in deuterium plasma with asymmetric ICRF: Pulse No: 51645 (–90^O phasing) and 51646 (+90^O phasing). Comparison of the relative γ-ray intensity recorded with detector viewing through the centre of plasma and in tangential direction.

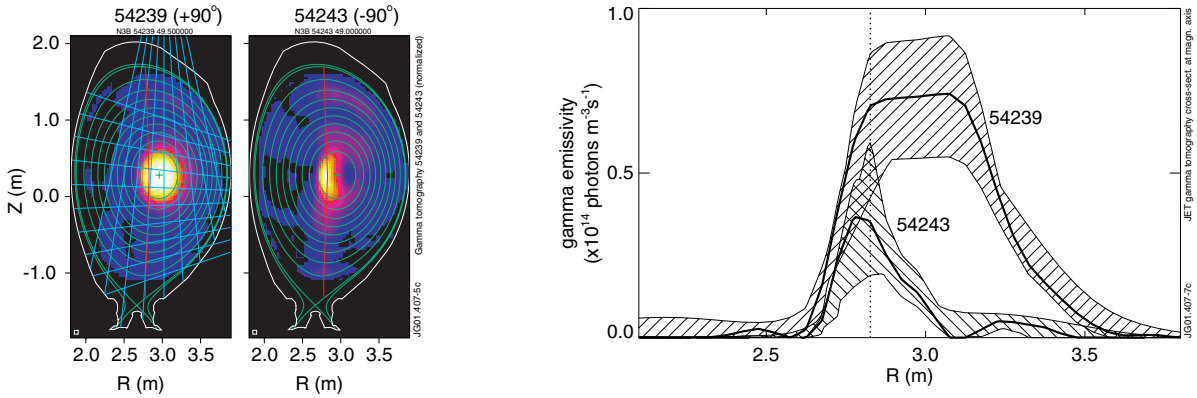

Figure 3: a) Comparison of the reconstructed emission profiles (normalised to the peak values) of γ-ray emissivity in the energy range 1.8–6 MeV for the two Pulse Nos: 54239 and 54243. Left: the lines of sight of the diagnostic are indicated by blue lines. A number of flux surfaces (from EFIT) are draw in green; the magnetic axis is indicated by a cross. The location of the resonance layer is indicated by a red line. The box in the lower-left corner indicates the grid size used in the tomographic reconstructions.

b) Cross-sections of reconstructed γ-ray emissivity along the major radius. The most reasonable reconstructions are shown by solid lines, and regions of uncertainty, determined by the method described in [11], are indicated by a shaded bands. The location of the resonance layer is given by a dotted line.

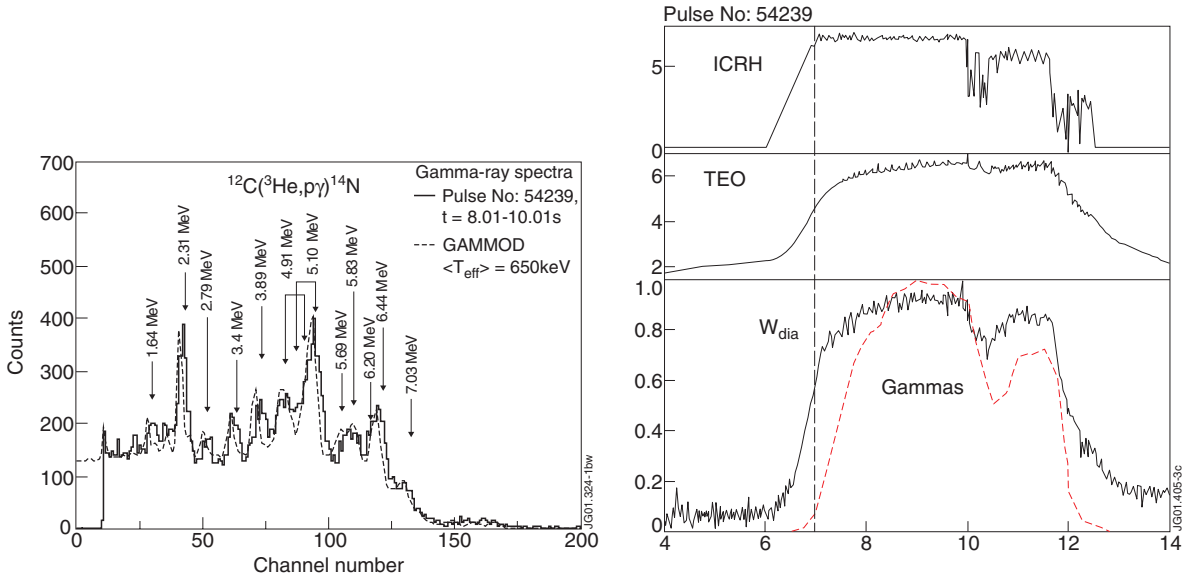

Figure 4: Left: experimental and calculated γ-ray spectra for Pulse No: 54239. Right: comparison of neutron and γ-ray rates behaviour during the discharge.

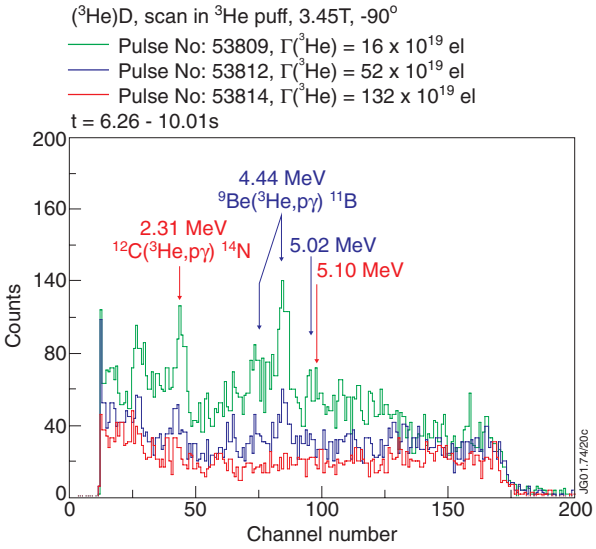

Figure 5: Gamma ray spectra measured in three discharges at different levels of ^{3}He-puff.

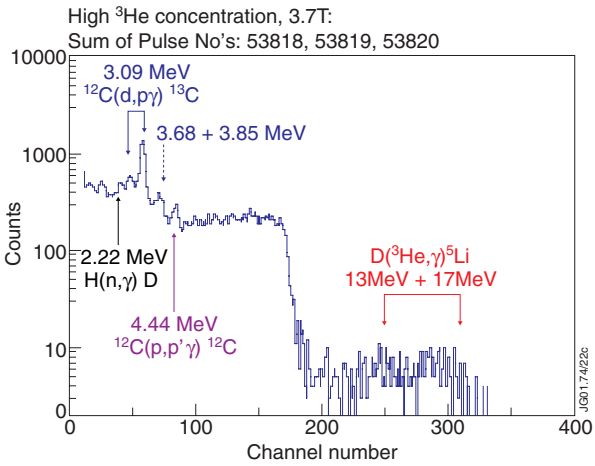

Figure 6: Gamma ray spectrum recorded during three discharges at high ^{3}He density and toroidal field 3.7T.

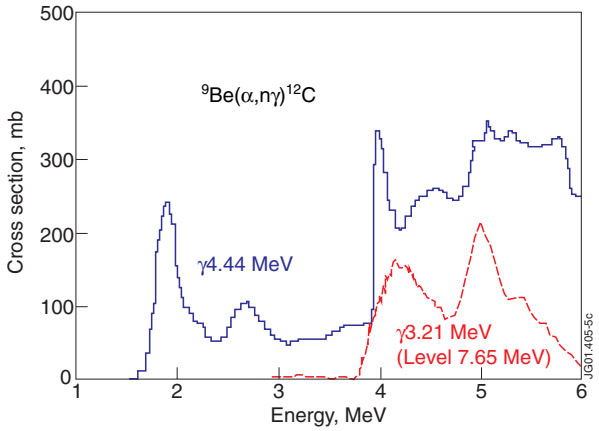

Figure 7: Excitation functions of 4.44MeV and 7.65MeV level of ^{12}C in reaction $^{9}Be(\alpha,n\gamma)^{12}C$.

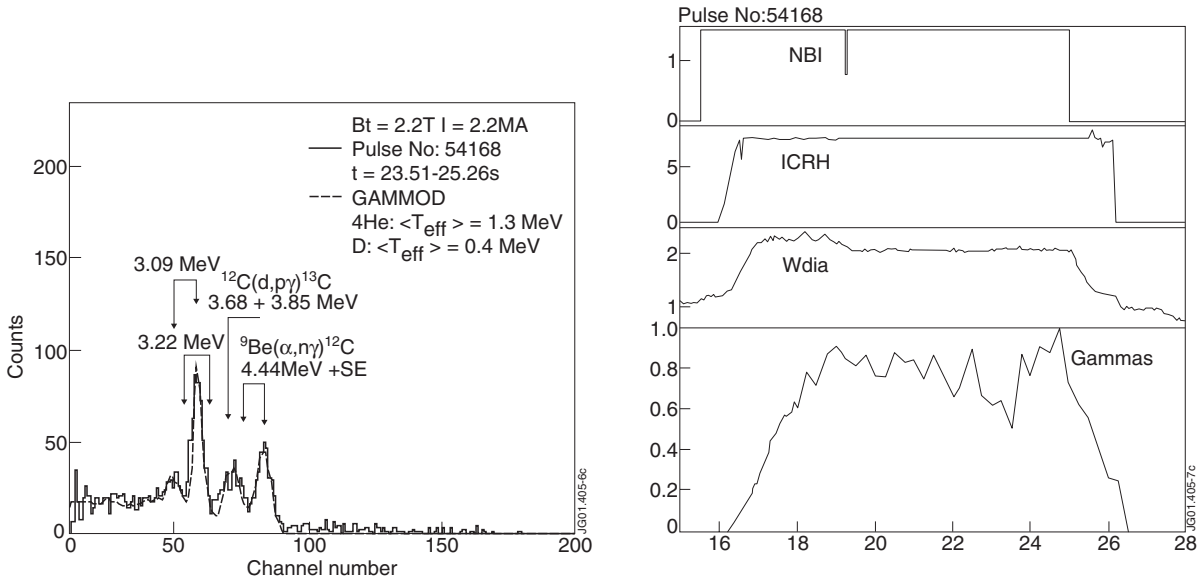

Figure 8: Left: experimental and calculated γ-ray spectra for Pulse No: 54168.
Right: comparison of neutron and 4.44-MeV γ-ray rates behaviour during the discharge.

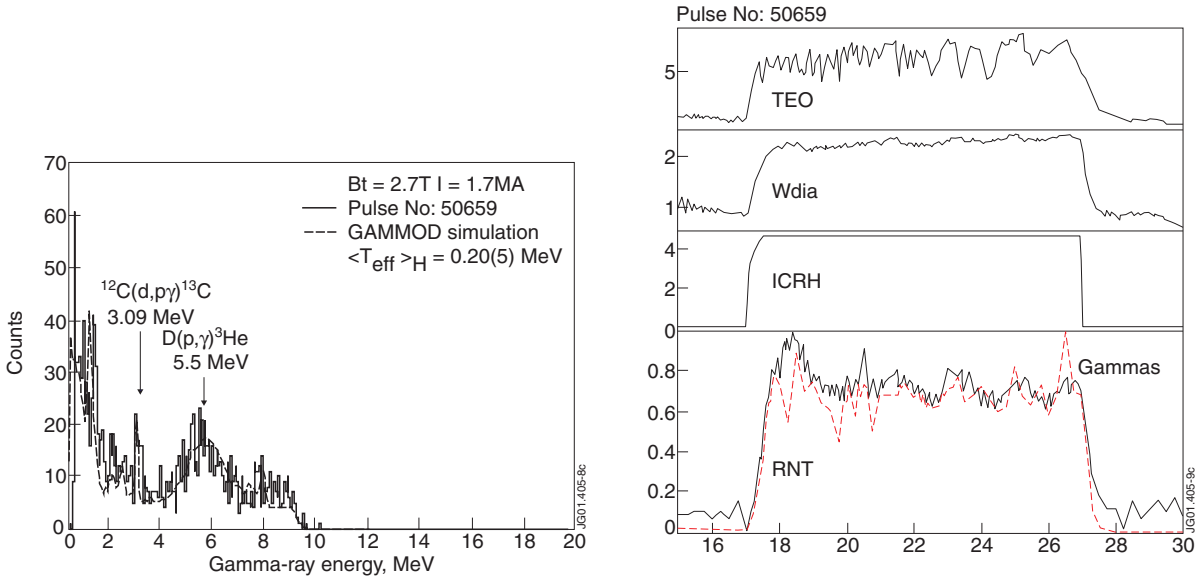

Figure 9: Left: experimental and calculated γ-ray spectra for Pulse No: 50659. Right: comparison of neutron and γ-ray rates behaviour during the discharge.

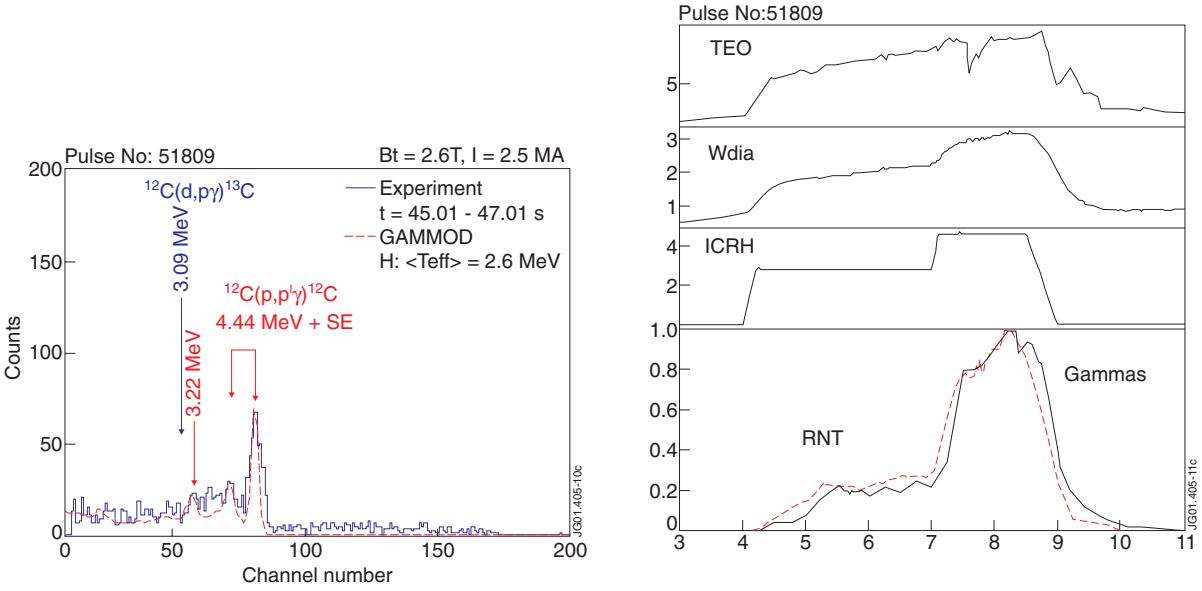

Figure 10: Left: experimental and calculated γ-ray spectra for Pulse No: 51809. Right: comparison of neutron and γ-ray rates behaviour during the discharge.

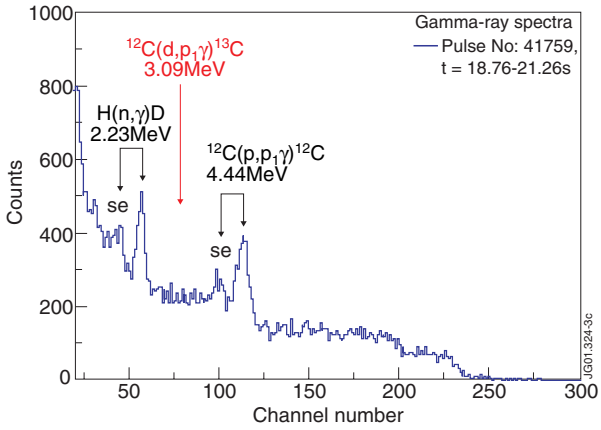

Figure 11: Gamma ray spectra recorded in D-T discharge with H-minority heating.